Polar boundary layer bromine explosion and ozone depletion events in the chemistry-climate model EMAC v2.52: Implementation and evaluation of AirSnow algorithm

Stefanie Falk[1,a] and Björn-Martin Sinnhuber[1]

[1]Institute of Meteorology and Climate Research, Karlsruhe Institute of Technology, Karlsruhe, Germany
[a]now at: Department of Geosciences, University of Oslo, Oslo, Norway

Correspondence to: Björn-Martin Sinnhuber (bjoern-martin.sinnhuber@kit.edu)

Abstract. Ozone depletion events (ODE) in the polar boundary layer have been observed frequently during spring-time. They are related to events of boundary layer enhancement of bromine. Consequently, increased vertical column densities (VCD) of BrO have been observed from satellites. These so called bromine explosion events have been discussed serving as source of tropospheric BrO at high latitudes. We have implemented a treatment of bromine release and recycling on sea ice and snow covered surfaces in the global chemistry-climate model EMAC (ECHAM/MESSy Atmospheric Chemistry) based on the scheme of Toyota et al. (2011). In this scheme, dry deposition fluxes of HBr, HOBr, and $\mathrm{BrNO_3}$ over ice and snow covered surfaces are recycled into $\mathrm{Br_2}$ fluxes. In addition, dry deposition of $\mathrm{O_3}$, dependent on temperature and sunlight, triggers a $\mathrm{Br_2}$ release from surfaces associated with first-year sea ice. Many aspects of observed bromine enhancements and associated episodes of near-complete depletion of boundary layer ozone, both in the Arctic and in the Antarctic, are reproduced by this relatively simple approach. We present first results from our global model studies extending over a full annual cycle, including comparisons with GOME satellite BrO VCD and surface ozone observations.

1 Introduction

Events of near-complete depletion of polar boundary layer ozone are observed frequently during spring-time over both hemispheres (Oltmans, 1981; Barrie et al., 1988; Bottenheim et al., 1986, 2002, 2009). Individual events typically last between several hours to a few days. The boundary layer ozone depletion events (ODE) are almost certainly related to events of strongly enhanced bromine, so called bromine explosion events. Enhanced bromine monoxide (BrO) column densities are regularly observed from satellites over both hemispheres, predominantly over the marginal sea ice zone, but sometimes also over inland ice and snow covered regions (e.g., Richter et al., 1998). In addition to their impact on boundary layer ozone, bromine explosion events play an important role in mercury deposition and corresponding environmental impacts (Lindberg et al., 2002; Stephens et al., 2012). Proposed mechanisms for bromine explosion events involve frost flowers on thin sea ice (Kaleschke et al., 2004) and blowing of saline snow on sea ice (Yang et al., 2010). Carbonate precipitation in brine at low temperatures has been suggested as efficient release trigger of sea salt bromine to the atmosphere (Sander et al., 2006). However, measurements of $\mathrm{Br_2}$ release in dependence of illumination and ozone volume mixing ratio (VMR) from various types of snow and

ice indicate that neither sea ice itself nor brine icicles are a major source for Br_2 but in addition to snow on sea ice also snow on land surfaces has to be taken into consideration (Pratt et al., 2013). Recent reviews on the subject are provided by Simpson et al. (2007), Saiz-Lopez and von Glasow (2012), Abbatt et al. (2012), and Custard et al. (2015). There has been considerable progress in describing the mechanisms involved in bromine release and boundary layer ODE based on field measurements and laboratory experiments. Regarding the underlying heterogeneous chemical reactions, many similarities can be drawn between the very cold and hostile polar boundary layer and the polar upper troposphere - lower stratosphere (UTLS), where polar stratospheric clouds (PSCs) play a major role in halogen activation. In these cold regimes, icy surfaces allow or accelerate reactions which are impossible or rather slow in gas phase chemistry. For sustaining catalytic ozone depletion, the activation of halogens through heterogeneous reactions is very important. While mainly chlorine is activated in PSCs, bromine activation is favored by the processes taking place in the polar boundary layer. In the following we will give an account of the review article by Abbatt et al. (2012). Accordingly, the existing modeling approaches can be grouped into four categories:

- Frost flowers ($\rightarrow$ sea salt aerosol formation),
- bulk ice and snow ($\rightarrow Br_2$ release),
- blowing of saline snow ($\rightarrow$ uplifting of sea salt and aerosol formation), and
- snowpack (photo)chemistry ($\rightarrow Br_2$ release).

Frost flowers covered in high saline brine, are sturdy while fragile in appearance and contribute less to saline aerosol formation and bromine explosion events than originally anticipated (Domine et al., 2005). Br^- enriched brine is formed on sea ice through drainage and precipitation of hydrohalite ($NaCl \cdot 2H_2O$) at temperatures below 251 K (Abbatt et al., 2012, and references therein). In the course of summer, most salt is washed out from sea ice. Therefore, multi-year sea ice can be discarded as source of bromine explosion events. In contrast to solutions, acidity is not important on icy surfaces (Adams et al., 2002). Since $HOBr$ is rather rapidly reacting forming Br_2, the rate of Br_2 release is mainly limited by mass transfer from the atmosphere to snow or ice (Huff and Abbatt, 2000). Apart from the complex heterogeneous photochemistry taking place in a quasi-liquid phase on ice grains in the snowpack (Thomas et al., 2011; Pratt et al., 2013), ozone itself has the capacity of triggering auto-catalytic reactions by oxidizing bromine already before polar sunrise.

On the basis of empirical and modeling results, Toyota et al. (2011) presented a parameterization of Br_2 release from bulk ice and snow within the Global Environmental Multiscale model with Air Quality processes (GEM-AQ). GEM-AQ is based on Canada's operational weather prediction model developed by the Meteorological Services of Canada (MSC) for the interaction of atmospheric chemistry with sea ice and snow surfaces. This parameterization reproduces many aspects of observed bromine enhancements and boundary layer ODE.

Here we present an implementation of a mechanism based on the work of Toyota et al. (2011) into the ECHAM/MESSy Atmospheric Chemistry (EMAC) model (Jöckel et al., 2010). The mechanism and its integration into the existing submodel ONEMIS (Kerkweg et al., 2006) are described in Sect. 2. In Sect. 3, results from several one year long integrations of the model with and without bromine release are presented and compared to surface ozone observations as well as observations of

BrO vertical column density (VCD) from the Global Ozone Monitoring Experiment (GOME) satellite instrument on board ERS-2 (Richter et al., 1998, 2002). We show that many aspects of observations regarding BrO enhancements and ODE are reproduced by this mechanism without any further tuning of parameters. Unlike most previous modeling studies, we do not focus on Arctic spring time only but investigate a full annual cycle on both hemispheres.

2 Model and experiments

The EMAC model is a numerical chemistry-climate model, based on 5th generation European Centre Hamburg general circulation model (ECHAM5) (Roeckner et al., 2006) as dynamical core. Various submodels describe atmospheric and Earth system processes and are coupled via the Modular Earth Submodel System (MESSy) (Jöckel et al., 2005). MESSy provides an infrastructure with generalized interfaces for control and coupling of components. Further information about MESSy and EMAC is available from the MESSy project homepage. MESSy enables for a flexible handling of emissions in EMAC, e.g., prescribed fluxes, concentrations of tracers at the boundary layer or any other given level, and emissions dependent on dynamical atmospheric fields. Latter are treated as online emissions using the submodel ONEMIS (Kerkweg et al., 2006). ONEMIS provides facility functions for flux to tracer concentration conversions. According to the MESSy philosophy, ONEMIS is separated into a submodel interface layer (SMIL) for unified data handling among different submodels and an implementation layer of the actual emission mechanisms (submodel core layer, SMCL). A recap of the mechanism proposed by Toyota et al. (2011) (Sect. 2.1) and details about its integration into the EMAC model (Sect. 2.2) are given in the following. In Sect. 2.3, scope and setup of a set of test experiments are summarized.

2.1 Description of the mechanism

It is assumed that at least part of the observed Br_2 flux originates from heterogeneous reactions on snow grains in the surface layer of a snowpack (Pratt et al., 2013). These snow grains are considered coated by a Br^- enriched film of liquid water and show a distinct acidity. In this quasi-liquid phase, heterogeneous reactions of $HOBr$ and $BrNO_3$ with either Br^- and Cl^- can take place:

$$HOBr + Br^- \xrightarrow{H^+} Br_2 + H_2O, \tag{R1}$$

$$BrNO_3 + Br^- \rightarrow Br_2 + NO_3^-, \tag{R2}$$

$$HOBr + Cl^- \xrightarrow{H^+} BrCl + H_2O, \tag{R3}$$

$$BrNO_3 + Cl^- \rightarrow BrCl + NO_3^-. \tag{R4}$$

Interhalogene reactions may convert $BrCl$ into Br_2:

$$BrCl + Br^- \leftrightarrow Br_2Cl^- \leftrightarrow Br_2 + Cl^- \tag{R5}$$

$BrCl$ is partly released to the atmosphere before undergoing this last reaction. In addition, various photochemical gas-, aqueous-, and heterogeneous-phase reactions are taking place in the top layer of a snowpack (for details see, e.g., Pratt et al., 2013, Fig. 2), which are rather similar to heterogeneous reactions occurring on PSCs. A list of heterogeneous reactions involving bromine included in MECCA is provided as Supplement S.1. Another reaction pathway oxidizing bromine is triggered by ozone dry deposition without the influence of sunlight. Three surface types, first-year sea ice (FY), multi-year sea ice (MY), and snow on land (LS) are differentiated. In any case, the respective surface temperature has to be below a temperature threshold T_{crit}. The critical conversion of a dry deposition flux of ozone (Φ_{O_3}) into an emission flux of Br_2 (or $BrCl$) is moderated by an ad hoc molar yield Φ_1, dependent on surface type and illumination. Toyota et al. (2011) have parametrized these heterogeneous reaction pathways ($HOBr$ / $BrNO_3$ / $O_3 \rightarrow Br_2$) in a simple way taking state-of-the-art knowledge into account:

$$\Phi_1 = \begin{cases} 0.001 & \text{if } \textit{dark} \text{ FY}, \\ 0.075 & \text{if } \textit{sunlit} \text{ FY}, \\ 0 & \text{if MY or LS}. \end{cases} \tag{1}$$

I.e., on FY sea ice, only 0.1% of the dry deposition of O_3 will be converted into Br_2 in case the surface is not sunlit (sun's zenith angle above $\theta_{\mathrm{crit}} = 85\,^\circ$), otherwise 7.5% is converted. No release of Br_2 from MY sea ice or LS is assumed. The specific value of Φ_1 has been obtained as best choice by cross-validating modeling results with observed spring-time boundary layer ozone data at Alert, Barrow, and Zeppelin (Toyota et al., 2011, Section 3.1).

The conversion of dry deposition fluxes of $HOBr$ (Φ_{HOBr}), $BrNO_3$ (Φ_{BrNO_3}), and HBr (Φ_{HBr}) is considered independent of illumination. In case of FY sea ice, the snowpack on top is regarded as an infinite pool of Br^- and Cl^-. The sum of $HOBr$ and $BrNO_3$ dry deposition fluxes ($\Phi_{HOBr} + \Phi_{BrNO_3}$) is fully recycled into Br_2. In case of MY sea ice, only the Cl^- pool remains infinite, for Cl^- is about 2 to 3 orders of magnitude more abundant in snow than Br^- (Toyota et al., 2011). The release of Br_2 depends on $\Phi_{HOBr} + \Phi_{BrNO_3}$ in comparison to the dry deposition flux of HBr. If $\Phi_{HOBr} + \Phi_{BrNO_3}$ was less than Φ_{HBr} a full conversion of $\Phi_{HOBr} + \Phi_{BrNO_3}$ to Br_2 is assumed. Otherwise, only half of the difference $\Phi_{HOBr} + \Phi_{BrNO_3} - \Phi_{HBr}$ is recycled to Br_2, the other half is converted to $BrCl$. For LS, neither Br^- nor Cl^- is available unlimited. Hence, only the smaller of $\Phi_{HOBr} + \Phi_{BrNO_3}$ and Φ_{HBr} is converted to Br_2. The resulting *yield* is summarized in Φ_2:

$$\Phi_2 = \begin{cases} 1 & \text{if FY}, \\ 0.5 - 1 & \text{if MY}, \\ 0 - 1 & \text{if LS}. \end{cases} \tag{2}$$

Schematically, all release scenarios are shown in Fig. 1 (adapted from Fig. 1 of Toyota et al. (2011)). Herein, black arrows denote dry deposition of $HOBr$, $BrNO_3$, HBr, and O_3. Blue doted arrows indicate gas-phase photochemistry. The recycled fluxes are displayed by dashed orange (O_3) and red ($HOBr$, $BrNO_3$, HBr) arrows.

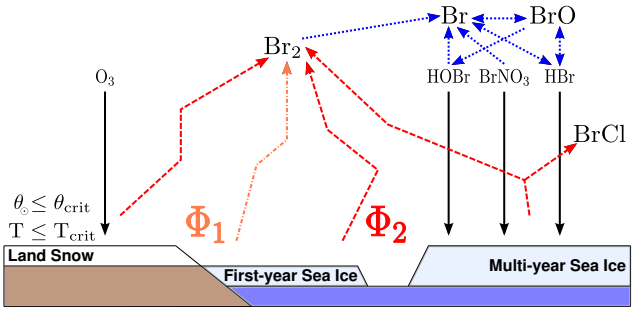

Figure 1. Schematic scenario of bromine release from first-year sea ice, multi-year sea ice, and land snow adapted from Toyota et al. (2011) for a temperature threshold T_{crit}. Black arrows denote dry deposition of HOBr, $BrNO_3$, HBr, and O_3. Blue doted arrows indicate gas-phase photochemistry. Dry deposition fluxes are recycled into Br_2 with respect to a molar yield Φ_1 in case of O_3 (dashed orange) and Φ_2 in case of the brominated species (dashed red).

2.2 Implementation

In accordance to the described scheme, submodel interface layer (SMIL), submodel core layer (SMCL), and namelist of ONEMIS have been extended based on EMAC version 2.52. Channel objects, used by a subroutine `airsnow_emissions` (implemented in SMCL), include surface temperature (`tsurf`), fraction of snow cover on land (`cvs`), fraction of ice cover on ocean (`seaice`), cosine of sun's zenith angle (`cossza`), and dry deposition fluxes of HOBr, $BrNO_3$, HBr, and O_3 (`drydepflux_<HOBr, BrNO3, HBr, O3>`). Dry deposition is computed by submodel DDEP (formerly DRYDEP, Kerkweg et al., 2006, b). In the SMIL of ONEMIS, these channel objects are defined and initialized and the subroutine `airsnow_emissions` is called. Additional information about multi-year sea ice cover (MYSIC) has to be provided through data import. Currently, we are using a MYSIC estimate based on mean SIC from ERA-Interim (see Section 2.3). Steering parameters, Φ_1, T_{crit}, and θ_{crit}, can be changed in the corresponding control sequence within the ONEMIS namelist file. However, the parameter relevant to MY sea ice and LS in Φ_1 is currently not used, since no parameterization has been provided by Toyota et al. (2011). New output channels `snow_air_flux_br2` and `snow_air_flux_brcl` have been defined in the SMIL of ONEMIS. More detail of the algorithm implemented in the subroutine `airsnow_emissions` is provided as Nassi-Shneiderman diagram in Supplement S.2. The new emission mechanism has been named *AirSnow* and can be switched on in the ONEMIS namelist – an example excerpt has been added as Supplement S.3. After Br_2 has been released, we make use of atmospheric bromine chemistry that is identical to EMAC's standard stratospheric bromine chemistry (Supplement S.1).

2.3 Validation Experiments

Three experiments have been performed using EMAC version 2.52 (see Table 1 for a summary). The basic model setup has been adapted from RC1SD-base-08, which is part of a Chemistry Climate Model Initiative (CCMI) recommended set of simulations by the Earth System Chemistry integrated Modelling (ESCiMo) consortium (Jöckel et al., 2016). The model integrations use specified dynamics nudged to ERA-Interim for the year 2000. Accordingly, ERA-Interim sea ice cover (SIC) has been used.

Table 1. EMAC model experiments used in this study. All experiments have been done using specified dynamics nudged to ERA-Interim. Accordingly, ERA-Interim SIC has been used. The setup is based on the consortial ESCiMo simulation RC1SD-base-08. Experiments have been performed for an assumption of first-year sea ice only (FYSIC) and for a multi-year sea ice cover (MYSIC) estimated from SIC. The temperature threshold for all simulations has been $T_{\mathrm{crit}} = -15\,^{\circ}\,\mathrm{C}$, accordingly.

Experiment	Model Version	Resolution	Time-Span	Chemistry	VSLS Emission	AirSnow	$r_{\mathrm{O_3}}^{\mathrm{ice-snow}}$
BrXplo_ref	2.52	T42L90MA	Jan–Dec 2000	full	AIRSEA	no	$1/2000\,\mathrm{sm}^{-1}$
BrXplo_fysic	2.52	T42L90MA	Jan–Dec 2000	full	AIRSEA	FYSIC	$1/2000\,\mathrm{sm}^{-1}$
BrXplo_mysic	2.52	T42L90MA	Jan–Dec 2000	full	AIRSEA	MYSIC	$1/2000\,\mathrm{sm}^{-1}$
BrXplo_mysic_rs	2.52	T42L90MA	Jan–Dec 2000	full	AIRSEA	MYSIC	$1/10000\,\mathrm{sm}^{-1}$

The chosen spatial resolution is T42L90MA corresponding to a $2.8^{\circ} \times 2.8^{\circ}$ grid, with a top level at 0.01 hPa and distributed to 90 levels. Output has been saved with 1-hourly temporal resolution. In contrast to RC1SD-base-08, fluxes of brominated very short-lived substances (VSLS), $\mathrm{CH_2Br_2}$ and $\mathrm{CHBr_3}$, are computed online from sea water concentrations (Ziska et al., 2013) using the EMAC submodel AIRSEA (Pozzer et al., 2006) as described by Lennartz et al. (2015). In this scheme, sea ice acts as a lid blocking the emission of VSLS to the atmosphere. Comprehensive tropospheric and stratospheric chemistry as well as heterogeneous reactions within MECCA (Sander et al., 2011) have been activated for an aerosol surface area concentration climatology.

The basic parameter setup has been adopted without changes as proposed by Toyota et al. (2011). The temperature threshold for all simulations has been $T_{\mathrm{crit}} = -15\,^{\circ}\,\mathrm{C}$, accordingly.

In EMAC no discrimination is made between FY sea ice and MY sea ice, therefore we initially assume all ice to be first-year (BrXplo_fysic). A multi-year sea ice cover has been computed from RC1SD-base-08 10-hourly SIC output based on ERA-Interim. We regard ice at a fixed location that survived one melting season as multi-year. Hence for simplicity, we assume no drift of ice masses. SIC has been integrated for respective summer months on northern (August/September) and southern (February/March) hemisphere. The SIC at the minimum of the integrated SIC has been chosen as MYSIC for the respective year after. The resulting MYSIC for the year 2000 are shown in Fig. 2 together with monthly mean SIC for April (northern hemisphere) and September (southern hemisphere). The result is very similar with regard to patterns and extend of MYSIC on maps retrieved from satellite observation (US National Snow & Ice Data Center (NSIDC), 2017). Based on the MYSIC estimate, a second model integration (BrXplo_mysic) has been conducted. For comparison, a reference simulation with bromine release mechanism switched off has been done (referred to as BrXplo_ref). In a further sensitivity simulation, we have decreased the dry deposition of ozone over snow covered regions as proposed by Helmig et al. (2007) by changing the surface resistance in DDEP for ozone on snow and ice surfaces from the value of $r_{\mathrm{O_3}}^{\mathrm{ice-snow}} = 1/2000\,\mathrm{sm}^{-1}$ (Wesely, 1989) to $r_{\mathrm{O_3}}^{\mathrm{ice-snow}} = 1/10000\,\mathrm{sm}^{-1}$ (Helmig et al., 2007).

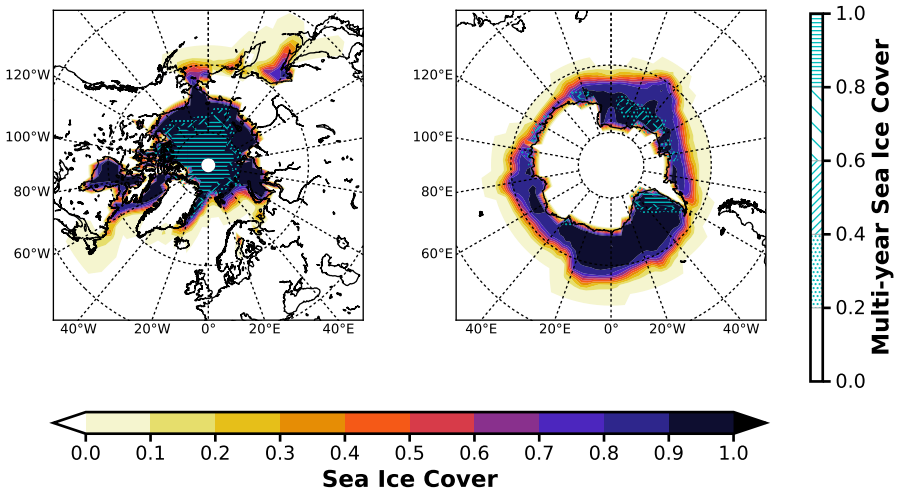

Figure 2. Sea ice cover fraction and estimated multi-year sea ice cover fraction for the year 2000. Mean SIC are shown for April on the northern hemisphere and September on the southern. MYSIC has been computed from RC1SD-base-08 10-hourly SIC based on ERA-Interim. For simplicity, we assume ice that survived one melting season as multi-year. (left) Northern hemisphere; (right) Southern hemisphere.

3 Results

In this section, we compare our simulations' results with observational data. For Br_2, which has been released from ice and snow, is transformed into BrO photolytically, enhancements of Br_2 lead to an increase of the BrO vertical column density. These enhancements have been observed by satellite instruments (e.g., Richter et al., 1998). At first, we compare the spatial distribution of BrO total VCD as simulated with EMAC (BrXplo_mysic) with GOME retrieved total VCD in both hemispheres. Implications on depletion events of surface ozone will be drawn in comparison to observational data at several ground-based sites in both hemispheres.

3.1 Total BrO vertical column density

Monthly mean GOME VCD retrieval of BrO subtracted by corresponding zonal means are shown in Fig. 3a) for both, northern and southern polar regions in April and September, respectively. The associated zonal means are available as Supplement S.5.1. In April, GOME data display a strong enhancement of BrO VCD across the whole coastal region of the Arctic ocean, except for the coast of Greenland. Hotspots can be found down the Hudson Bay, east of Novaya Zemlya, and around Hokkaido. There are only slight enhancements in the Antarctic coastal regions, but data are sparse. In September, enhancements around Antarctica can be in particular observed in the Ross and Weddell sea areas.

From 1-hourly BrO profiles of the EMAC model output, a total VCD has been integrated and re-sampled to 10–11 am local solar time, according to the ERS-2 equator crossing time of 10.30 am local time. In general, transition times at high latitudes differ from the equator crossing time due to satellite orbit. Differences in local local time may account for part of the differences

seen in the BrO comparison. The re-sampled data has been averaged monthly. As there is an offset between EMAC and GOME BrO VCD, we are showing anomalies here. The zonal mean BrO VCD has been subtracted to highlight the bromine explosion events. The associated zonal mean BrO data are show as Supplement S.5.2. The resulting EMAC total BrO VCD are shown in Fig. 3b). In comparison to GOME data, spatial patterns of BrO VCD are reasonably well reproduced by EMAC in the northern hemisphere in April. Only westward from Hudson Bay and eastward from Novaya Zemlya, respectively, no BrO enhancement is found in our simulation. The Hokkaido hotspot appears slightly shifted northward. In September, both observation and model, agree well in both hemispheres. In April, satellite data of Antarctica are too sparse to identify the hotspots that occur in the simulation.

A full overview of monthly mean total BrO VCD for both, observation and model, including all months has been added as Supplement S.4. In the northern hemisphere, the implemented mechanism is prone for BrO VCD enhancements shifted to early winter compared to GOME retrievals. In late spring and early summer, however, too few BrO is formed in the model. This may hint to sources of BrO in the Arctic which are not represented by this mechanism or an adherence to the chosen parameters. Further studies would be needed to resolve the source of this discrepancy. In the southern hemisphere, the modeled BrO enhancements in, e.g., August and September are similar in their occurrence, while the sparseness of GOME data in austral winter does not permit further conclusions regarding the quality of the parameterization in this region. Taking a look at the zonally averaged total BrO VCD (Supplement S.5), we find, that the modeled BrO VCD is generally too small in polar summer compared to observation by about $(1-4)\cdot 10^{13}\,\mathrm{molecules\,cm^{-2}}$ in both hemispheres, respectively. A better agreement between observation and model is achieved in winter. This is due to the implementation of the bromine release mechanism (doted lines indicating the reference simulation). Hence, taking the bromine released from ice and snow into account the overall model performance is enhanced with respect to polar BrO observation.

3.2 Ozone depletion events

Regarding depletion events of surface ozone, four different observation sites have been chosen on each hemisphere for comparison (Table 2). No data for Arrival Heights and Palmer Station have been available in 2000. For these stations, we show model results only. Time series of surface ozone VMR are shown in Figures 4–5 including both in situ observations (where available) and model simulations. For each simulation, the nearest grid point has been chosen as representative. In general, we find a good agreement between BrXplo_ref and observations for seasons without bromine release from ice and snow, except for Summit, South Pole station, and Neumayer station in austral winter, where model results are systematically lower compared to observations. In case of BrXplo_fysic all northern hemispheric sites display depletion events in spring as well as in fall. While the depletion events are not entirely in temporal coincidence with observed events, their frequency is generally well reproduced. However, events of ozone depletion in fall are not present in observation data. For Zeppelin Mountain and Alert, these *fault events* are due to the FYSIC assumption. For a decent multi-year sea ice cover is implemented in BrXplo_mysic, they vanish. In case of Barrow, a closer look into spring reveals an astonishing temporal as well as quantitative coincidence of surface ozone VMR especially in April (Fig. 5). The apparent *wiggles* are partly due to hard trigger thresholds T_{crit} and θ_{crit}, but similar structures are in fact apparent in the surface ozone observations at Barrow implying a diurnal variation of $\mathrm{O_3}$

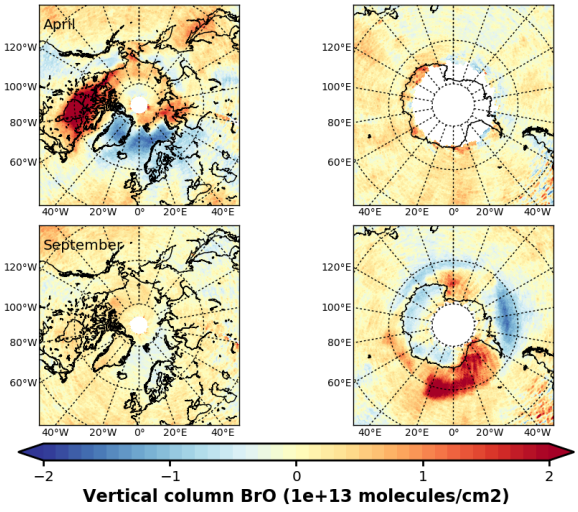

(a) GOME

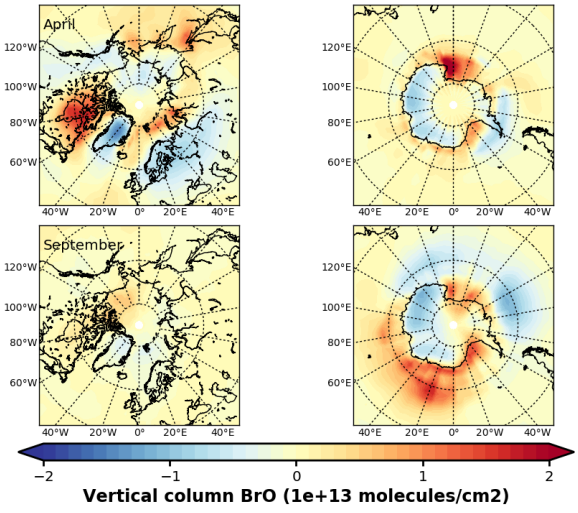

(b) EMAC

Figure 3. Anomalies of monthly mean VCD of BrO for the Arctic and Antarctic (April and September) with respect to monthly averaged zonal mean (see Supplement S.5), respectively. EMAC data have been sampled in accordance to local solar time 10–11 am. (a) GOME; (b) EMAC (BrXplo_mysic).

depletion. At Alert, our model does not capture the 2000s ODE that inflicted continuously low surface ozone levels for several days from late April until early May. As pointed out by Strong et al. (2002), this long-lasting depletion event was related to transport of ozone poor air originating from a region north of Ellesmere Island and the eastern arctic ocean, respectively. It is not clear whether transport of ozone depleted air masses or depletion itself is too weak in our simulation. At about the same time (late April, early May) observation displays a series of ODEs at Zeppelin mountain, which is also only partly reproduced

Table 2. Observation sites for surface ozone comparison. However, for Palmer station and Arrival Heights no observations of surface ozone are available for the year 2000, so that we present model results only for these two stations.

Site	Location	Latitude (°N)	Longitude (°E)	Altitude (m a.s.l.)	Data Provider
Alert	Canada	82.50	-62.30	210	EBAS (NILU)
Barrow	Alaska	71.32	-156.61	8	ESRL/GMD (NOAA)
Zeppelin Mountain	Spitsbergen	78.90	11.88	474	EBAS (NILU)
Summit	Greenland	72.54	-38.48	3238	ESRL/GMD (NOAA)
Palmer Station	Antarctica	-64.77	-64.05	21	*ESRL/GMD (NOAA)*
Neumayer Station	Antarctica	-70.68	-8.26	43	EBAS (NILU)
Arrival Heights	Antarctica	-77.85	166.78	22	*ESRL/GMD (NOAA)*
South Pole Station	Antarctica	-89.98	-24.8	2810	ESRL/GMD (NOAA)

by the model (e.g. on April 28th). Comparing observation and simulation in the southern hemisphere and Greenland, we find in general less ozone in BrXplo_mysic as well as in BrXplo_ref. This may hint to missing sources of polar ozone released from ice and snow in the model. Any analysis regarding the modeled occurrence of ODEs in the southern hemisphere is not affected by this. Despite the original mechanism's validation for northern hemispheric spring (Toyota et al., 2011), comparison of time series for the southern hemisphere do display ozone depletion events in a similar frequency as found in observational data. At Neumayer station, we find some events in late October and early November that might be coincidental, but in most cases simulated ODEs show up later than actually observed ODEs. In summary, while some aspects of ODEs are reproduced remarkably well by the implemented mechanism, especially the long-lasting event at Alert is not reproduced at all. This strongly hints to the involvement of further mechanisms, e.g., blowing snow and sea spray, in the depletion of polar surface ozone which have not yet been modeled in EMAC. In BrXplo_mysic_rs with the reduced dry deposition, ozone depletion events in fall and midwinter are suppressed and the agreement with observed ozone is generally improved (see Supplement S.6). Reducing the ozone dry deposition over snow and ice slightly increases boundary layer ozone at all discussed sites, but even with the reduced dry deposition the model significantly underestimates observed boundary layer ozone in Antarctica, indicating that other mechanisms exist that increase boundary layer ozone under these conditions (e.g., Oltmans, 1981; Helmig et al., 2007). A correlation between observed and modeled surface ozone at Barrow is shown in Fig. 6. (The supplementary information provides additional correlation plots for the other stations in the northern hemisphere, as well as additional plots for the sensitivity simulation with reduced ozone dry deposition.) As already evident from the time series in Fig. 5, low surface ozone values largely absent in the reference simulation are reproduced by the EMAC simulation including bromine explosion events, while some *fault events* are also generated, not present in the observations. Overall the linear correlation coefficients between modeled and observed ozone are improved by inclusion of the bromine explosion mechanism (from 0.008 to 0.21). A corre-

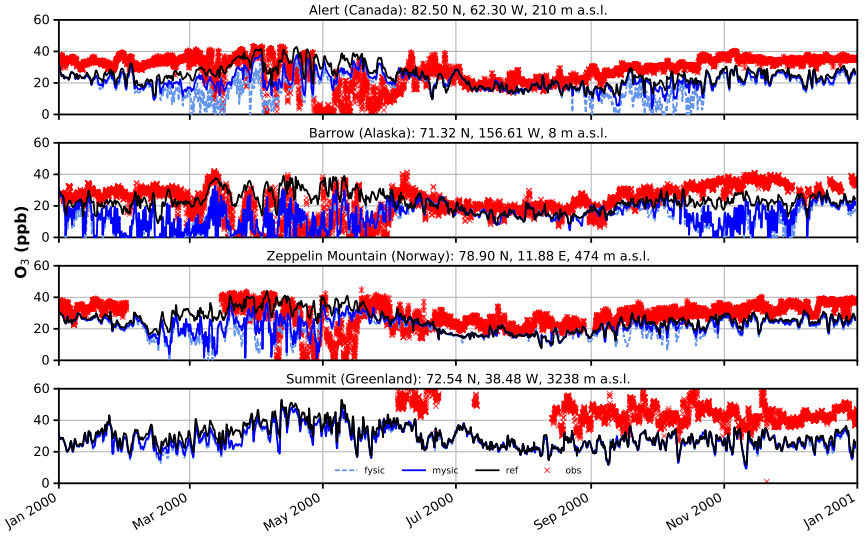

(a)

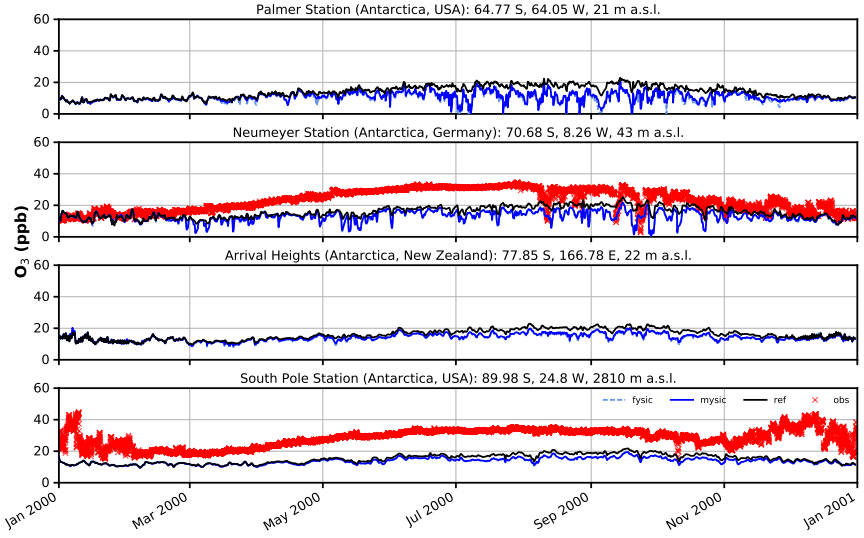

(b)

Figure 4. Surface ozone mixing ratios at four different observation sites. Comparison of in situ measurements (red crosses) with results from simulation (solid black – EMAC v2.52 default (no bromine explosions); light blue dashed – FYSIC; solid blue – MYSIC). Representatively, the nearest grid point has been chosen. (a) Northern hemisphere; (b) Southern hemisphere.

sponding lag correlation analysis shows that largest correlations are found for zero lag, with correlations falling to half of the maximum at about ± 2 days.

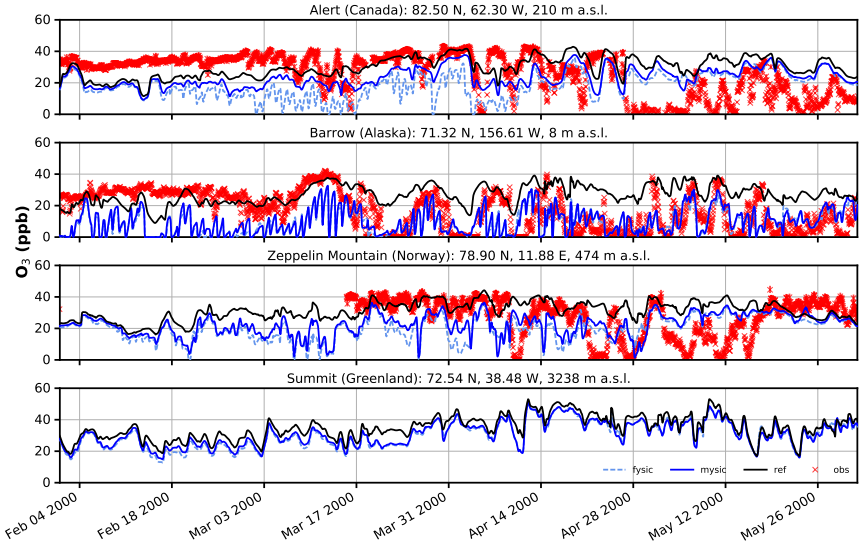

(a)

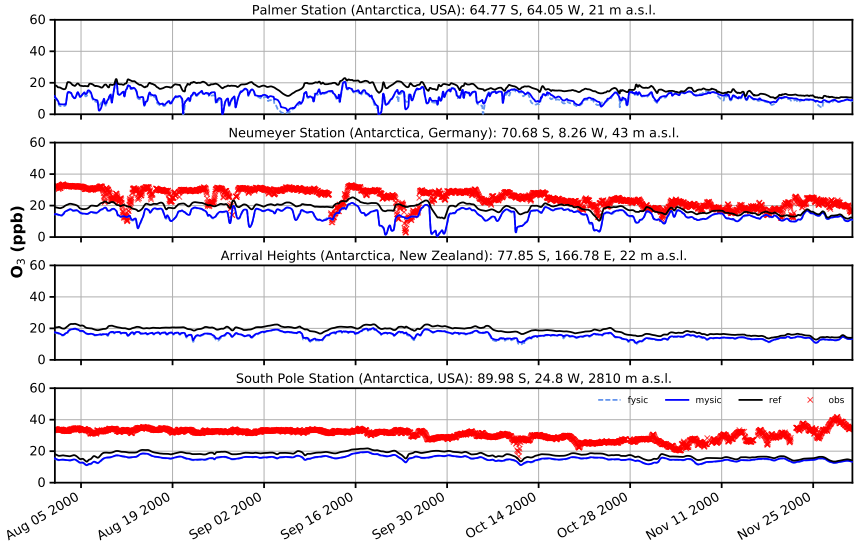

(b)

Figure 5. Surface ozone mixing ratios at four different observation sites for spring and austral spring, respectively. Comparison of in situ measurements (red crosses) with results from simulation (solid black – EMAC v2.52 default (no bromine explosions); light blue dashed – FYSIC; solid blue – MYSIC). Representatively, the nearest grid point has been chosen. (a) Northern hemisphere; (b) Southern hemisphere.

4 Discussion and conclusions

Many approaches describing bromine release in the polar regimes rely on modeling of complex micro physical processes which are too detailed for integration in a global chemistry-climate model. We have implemented a bromine release mechanism from

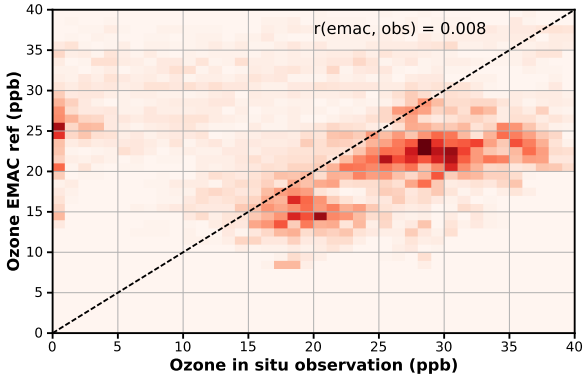

(a) BrXplo_ref

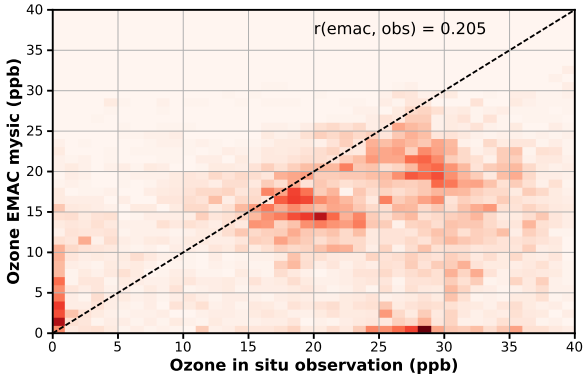

(b) BrXplo_mysic

Figure 6. Temporal correlation of modeled surface O_3 with observation at Barrow. Data have been binned in bins of 1 ppb width. While observed low ozone events at Barrow are absent in the reference simulation, in the BrXplo_mysic simulation there is now a population where both observation and model simultaneously show low ozone values, which is also reflected in the improved linear correlation coefficient from 0.008 to 0.21. (a) BrXplo_ref; (b) BrXplo_mysic.

sea ice and snow covered land surfaces based on the relatively simple parameterization suggested by Toyota et al. (2011) in the global chemistry-climate model EMAC. While the original study of Toyota et al. (2011) focused on Arctic spring time only, we extend the simulations to the global scale and a full annual cycle. We show that without any further tuning of the parameters, many aspects of observed polar bromine enhancements and boundary layer ozone depletion events are well reproduced by this mechanism within the EMAC model. Resulting spatial patterns of BrO total VCD and the temporal occurrence of surface ozone depletion events are comparable to BrO VCD retrieval of the GOME satellite instrument and in situ observation at different sites in both the Arctic and Antarctic, respectively. EMAC provides a wide range of Earth system related submodels and allows for simulations with full tropospheric and stratospheric (heterogeneous) chemistry in a selfconsistant manner. In our model integrations, inorganic bromine species (HBr, HOBr, $BrNO_3$) are provided in two ways: through photochemical transformation of organic source gases of natural and anthropogenic origin and through descending

stratospheric air containing inorganic bromine. The emission of bromine from very short-lived substances (CH_2Br_2, $CHBr_3$) is consistently computed online from sea water concentrations (Lennartz et al., 2015). The implemented bromine release mechanism relies on various assumptions which have been cross-validated with observations and are not entirely constrained. In particular, the dry deposition, which is one of the key factors in this bromine release mechanism, is still highly uncertain and hard to measure explicitly.

Our model simulations with this relatively simple mechanism successfully reproduce many observed features of bromine enhancement and ODEs (spatially as well as temporally), improving the overall model performance regarding BrO VCD and surface ozone concentrations at high latitudes. Although a lag analysis shows highest temporal correlation at zero lag between observation and model data at Barrow, there are still notable differences to other observations. In particular, there is a tendency to generate too high BrO columns and too many ODEs in mid winter and spring, which is reduced by decreasing the ozone dry deposition. The recognized ODE observed at Alert in 2000 is not at all reproduced by this bulk-snow-based mechanism. It is plausible, that in reality different processes, such as snowpack chemistry as well as bromine activation by blowing snow and sea spray, all play a role and contribute to the bromine explosion events at different sites. With the present work we have now a framework to further test these mechanisms in a global chemistry climate model.

Code availability. The Modular Earth Submodel System (MESSy) is continuously further developed and applied by a consortium of institutions. The usage of MESSy and access to the source code is licensed to all affiliates of institutions, which are members of the MESSy Consortium. Institutions can become a member of the MESSy Consortium by signing the MESSy Memorandum of Understanding. More information can be found on the MESSy Consortium Web-site (http://www.messy-interface.org). The modified code of the submodel ONEMIS described here will be made available with the next official release of the MESSy source code distribution.

Data availability. For any party interested, data can be made available on request.

Author contributions. Stefanie Falk has implemented the described mechanism, run and validated the simulations with observational data. Björn-Martin Sinnhuber suggested this study and took part in the analysis. Both authors contributed to the writing of the paper.

Competing interests. The authors declare that they have no conflict of interest.

Acknowledgements. Parts of this work were supported by the Deutsche Forschungsgemeinschaft (DFG) through the research unit 'SHARP' (SI1044/1-2), the German Bundesministerium für Bildung und Forschung (BMBF) through the project 'ROMIC-THREAT' (01GL1217B), and by the Helmholtz Association through its research program 'ATMO'.

Ozone in situ data for Alert, Neumayer station, and Zeppelin Mountain have been made available by the Norwegian Institute for Air Research. Database of observation data of atmospheric chemical composition and physical properties, EBAS. http://ebas.nilu.no. Data of Alert are provided by Environment Canada / Atmospheric Environmental Service (EC/AES), data of Neumayer station by Helmholtz-Zentrum Geestacht (HZG), and data of Zeppelin Mountain by Norwegian Institute for Air Research (NILU).

Ozone in situ data for Barrow, Summit, and South Pole station have been provided by U.S. Department of Commerce/National Oceanic & Atmospheric Administration (NOAA) – Earth System Research Laboratory – Global Monitoring Division. https://www.esrl.noaa.gov/gmd/ozwv/surfoz.

Tropospheric BrO column retrievals from GOME instrument have been provided in courtesy of Andreas Richter and John P. Burrows (University of Bremen). The data can be obtained from http://www.iup.uni-bremen.de/doas/gome_bro_data.htm.

We thank Andreas Richter and Astrid Kerkweg for helpful comments on an earlier version of the manuscript.

Thanks to Stefan Versick (KIT SimLab Climate and Environment) for technical support concerning the implementation into the EMAC model.

References

Abbatt, T. P. D., Thomas, J. L., Abrahamsson, K., Boxxe, C., Granfors, A., Jones, A. E., King, M. D., Saiz-Lopez, A., Shepson, P. B., Sodeau, J., Toohey, D. W.and Toubin, C., von Glasow, R., Wren, S. N., and Yang, X.: Halogene activation via interactions with environmental ice and snow in the polar lower troposphere amd other regions, Atmos. Chem. Phys., 12, 6237–6271, doi:10.5194/acp-12-6237-2012, 2012.

Adams, J. W., Holmes, N. S., and Crowley, J. N.: Uptake and reaction of HOBr on frozen and dry NaCl/NaBr surfaces between 253 and 233 K, Atmos. Chem. Phys., 2, 79–91, doi:10.5194/acp-2-79-2002, https://www.atmos-chem-phys.net/2/79/2002/, 2002.

Barrie, L. A., Bottenheim, J. W., Schnell, R. C., Crutzen, P. J., and Rasmussen, R. A.: Ozone destruction and photochemical reactions at polar sunrise in the lower Arctic atmosphere, Nature, 334, 138–141, doi:10.1038/334138a0, 1988.

Bottenheim, J. W., Gallant, A. G., and Brice, K. A.: Measutements of NOy Species and O-3 at 82-Degrees-N Latitude, Geophys. Res. Lett., 13, 113–116, doi:10.1029/GL013i002p00113, 1986.

Bottenheim, J. W., Fuentes, J. D., Tarasick, D. W., and Anlauf, K. G.: Ozone in the Arctic lower troposphere during winter and spring 2000 (ALERT2000), Atmos. Environ., 36, 2535–2544, doi:10.1016/S1352-2310(02)00121-8, 2002.

Bottenheim, J. W., Netcheva, S., Morin, S., and Nghiem, S. V.: Ozone in the boundary layer air over the Arctic Ocean: measurements during the TARA transpolar drift 2006-2008, Atmos. Chem. Phys., 9, 4545–4557, 2009.

Custard, K. D., Thompson, C. R., Pratt, K. A., Shepson, P. B., Liao, J., Huey, L. G., Orlando, J. J., Weinheimer, A. J., Apel, E., Hall, S. R., Flocke, F., Mauldin, L., Hornbrook, R. S., Poehler, D., General, S., Zielcke, J., Simpson, W. R., Platt, U., Fried, A., Weibring, P., Sive, B. C., Ullmann, K., Cantrell, C., Knapp, D. J., and Montzka, D. D.: The NOx dependence of bromine chemistry in the Arctic atmospheric boundary layer, Atmos. Chem. Phys., 15, 10 799–10 809, doi:10.5194/acp-15-10799-2015, 2015.

Domine, F., Taillandier, A. S., Simpson, W. R., and Severin, K.: Specific surface area, density and microstructure of frost flowers, Geophys. Res. Lett., 32, n/a–n/a, doi:10.1029/2005GL023245, http://dx.doi.org/10.1029/2005GL023245, l13502, 2005.

Helmig, D., Ganzeveld, L., Butler, T., and Oltmans, S. J.: The role of ozone atmosphere-snow gas exchange on polar, boundary-layer tropospheric ozone - a review and sensitivity analysis, Atmos. Chem. Phys., 7, 2007.

Huff, A. K. and Abbatt, J. P. D.: Gas-Phase Br2 Production in Heterogeneous Reactions of Cl2, HOCl, and BrCl with Halide-Ice Surfaces, J. Phys. Chem. A, 104, 7284–7293, doi:10.1021/jp001155w, http://dx.doi.org/10.1021/jp001155w, 2000.

Jöckel, P., Sander, R., Kerkweg, A., Tost, H., and Lelieveld, J.: Technical Note: The Modular Earth Submodel System (MESSy) - a new approach towards Earth System Modeling, Atmos. Chem. Phys., 5, 433–444, doi:10.5194/acp-5-433-2005, https://www.atmos-chem-phys.net/5/433/2005/, 2005.

Jöckel, P., Kerkweg, A., Pozzer, A., Sander, R., Tost, H., Riede, H., Baumgärtner, A., Gromov, S., and Kern, B.: Development cycle 2 of the Modular Earth Submodel System (MESSy2), Geosci. Model Dev., 3, 717–752, doi:10.5194/gmd-3-717-2010, http://www.geosci-model-dev.net/3/717/2010/, 2010.

Jöckel, P., Tost, H., Pozzer, A., Kunze, M., Kirner, O., Brenninkmeijer, C. A. M., Brinkop, S., Cai, D. S., Dyroff, C., Eckstein, J., Frank, F., Garny, H., Gottschaldt, K.-D., Graf, P., Grewe, V., Kerkweg, A., Kern, B., Matthes, S., Mertens, M., Meul, S., Neumaier, M., Nützel, M., Oberländer-Hayn, S., Ruhnke, R., Runde, T., Sander, R., Scharffe, D., and Zahn, A.: Earth System Chemistry integrated Modelling (ESCiMo) with the Modular Earth Submodel System (MESSy) version 2.51, Geosci. Model Dev., 9, 1153–1200, doi:10.5194/gmd-9-1153-2016, https://www.geosci-model-dev.net/9/1153/2016/, 2016.

Kaleschke, L., Richter, A., Burrows, J., Afe, O., Heygster, G., Notholt, J., Rankin, A. M., Roscoe, H. K., Hollwedel, J., Wagner, T., and Jacobi, H. W.: Frost flowers on sea ice as a source of sea salt and their influence on tropospheric halogen chemistry, Geophys. Res. Lett., 31, doi:10.1029/2004GL020655, 2004.

Kerkweg, A., Buchholz, J., Ganzeveld, L., Pozzer, A., Tost, H., and Jöckel, P.: Technical Note: An implementation of the dry removal processes DRY DEPosition and SEDImentation in the Modular Earth Submodel System (MESSy), Atmos. Chem. Phys., 6, 4617–4632, doi:10.5194/acp-6-4617-2006, http://www.atmos-chem-phys.net/6/4617/2006/, 2006.

Kerkweg, A., Sander, R., Tost, H., and Jöckel, P.: Technical note: Implementation of prescribed (OFFLEM), calculated (ONLEM), and pseudo-emissions (TNUDGE) of chemical species in the Modular Earth Submodel System (MESSy), Atmos. Chem. Phys., 6, 3603–3609, 2006.

Lennartz, S. T., Krysztofiak, G., Marandino, C. A., Sinnhuber, B.-M., Tegtmeier, S., Ziska, F., Hossaini, R., Krüger, K., Montzka, S. A., Atlas, E., Oram, D. E., Keber, T., Bönisch, H., and Quack, B.: Modelling marine emissions and atmospheric distributions of halocarbons and dimethyl sulfide: the influence of prescribed water concentration vs. prescribed emissions, Atmos. Chem. Phys., 15, 11 753–11 772, doi:10.5194/acp-15-11753-2015, http://www.atmos-chem-phys.net/15/11753/2015/, 2015.

Lindberg, S. E., Brooks, S., Lin, C. J., Scott, K. J., Landis, M. S., Stevens, R. K., Goodsite, M., and Richter, A.: Dynamic oxidation of gaseous mercury in the Arctic troposphere at polar sunrise, Envir. Sci. Tech., 36, 1245–1256, doi:10.1021/es0111941, 2002.

Oltmans, S. J.: Surface Ozone Measurements In Clean-Air, J. Geophys. Res.-Oceans Atmos., 86, 1174–1180, doi:10.1029/JC086iC02p01174, 1981.

Pozzer, A., Jöckel, P. J., Sander, R., Williams, J., Ganzeveld, L., and Lelieveld, J.: Technical note: the MESSy-submodel AIRSEA calculating the air-sea exchange of chemical species, Atmos. Chem. Phys., 6, 5435–5444, 2006.

Pratt, K. A., Custard, K. D., Shepson, P. B., Douglas, T. A., Pöhler, D., General, S., Zielcke, J., Simpson, W. R., Platt, U., Tanner, D. J., Huey, L. G., Carlsen, M., and Stirm, B. H.: Photochemical production of molecular bromine in Arctic surface snowpacks, Nat. Geosci., 6, 351–356, doi:10.1038/NGEO1779, 2013.

Richter, A., Wittrock, F., Eisinger, M., and Burrows, J. P.: GOME observations of tropospheric BrO in northern hemispheric spring and summer 1997, Geophys. Res. Lett., 25, 2683–2686, doi:10.1029/98GL52016, 1998.

Richter, A., Wittrock, F., Ladstatter-Weissenmayer, A., and Burrows, J. P.: GOME measurements of stratospheric and tropospheric BrO, in: REMOTE SENSING OF TRACE CONSTITUENTS IN THE LOWER STRATOSPHERE, TROPOSPHERE AND THE EARTH'S SURFACE: GLOBAL OBSERVATIONS, AIR POLLUTION AND THE ATMOSPHERIC CORRECTION, edited by Burrows, J. P. and Takeucki, N., vol. 29 of *Adv. Space. Res.*, pp. 1667–1672, Comm Space Res, doi:10.1016/S0273-1177(02)00123-0, A1 2 Symposium of COSPAR Scientific Commission A held at the 33rd COSPAR Scientific Assembly, WARSAW, POLAND, JUL, 2000, 2002.

Roeckner, E., Brokopf, R., Esch, M., Giorgetta, M., Hagemann, S., Kornblueh, L., Manzini, E., Schlese, U., and Schulzweida, U.: Sensitivity of simulated climate to horizontal and vertical resolution in the ECHAM5 atmosphere model, J. Climate, 19, 3771–3791, doi:10.1175/JCLI3824.1, 2006.

Saiz-Lopez, A. and von Glasow, R.: Reactive halogen chemistry in the troposphere, Chem. Soc. Rev., 41, 6448–6472, doi:10.1039/c2cs35208g, 2012.

Sander, R., Baumgaertner, A., Gromov, S., Harder, H., Jöckel, P., Kerkweg, A., Kubistin, D., Regelin, E., Riede, H., Sandu, A., Taraborrelli, D., Tost, H., and Xie, Z.-Q.: The atmospheric chemistry box model CAABA/MECCA-3.0, Geosci. Model Dev., 4, 373–380, doi:10.5194/gmd-4-373-2011, http://www.geosci-model-dev.net/4/373/2011/, 2011.

Sander, R., Burrows, J., and Kaleschke, L.: Carbonate precipitation in brine - a potential trigger for tropospheric ozone depletion events, Atmos. Chem. Phys., 6, 4653–4658, 2006.

Simpson, W. R., von Glasow, R., Riedel, K., Anderson, P., Ariya, P., Bottenheim, J., Burrows, J., Carpenter, L. J., Friess, U., Goodsite, M. E., Heard, D., Hutterli, M., Jacobi, H.-W., Kaleschke, L., Neff, B., Plane, J., Platt, U., Richter, A., Roscoe, H., Sander, R., Shepson, P., Sodeau, J., Steffen, A., Wagner, T., and Wolff, E.: Halogens and their role in polar boundary-layer ozone depletion, Atmos. Chem. Phys., 7, 4375–4418, 2007.

Stephens, C. R., Shepson, P. B., Steffen, A., Bottenheim, J. W., Liao, J., Huey, L. G., Apel, E., Weinheimer, A., Hall, S. R., Cantrell, C., Sive, B. C., Knapp, D. J., Montzka, D. D., and Hornbrook, R. S.: The relative importance of chlorine and bromine radicals in the oxidation of atmospheric mercury at Barrow, Alaska, J. Geophys. Res.-Atmos., 117, doi:10.1029/2011JD016649, 2012.

Strong, C., Fuentes, J. D., Davis, R. E., and Bottenheim, J. W.: Thermodynamic attributes of Arctic boundary layer ozone depletion, Atmos. Environ., 36, 2641–2652, doi:https://doi.org/10.1016/S1352-2310(02)00114-0, http://www.sciencedirect.com/science/article/pii/S1352231002001140, Air/Snow/Ice Interactions in the Arctic: Results from ALERT 2000 and SUMMIT 2000, 2002.

Thomas, J. L., Stutz, J., Lefer, B., Huey, L. G., Toyota, K., Dibb, J. E., and von Glasow, R.: Modeling chemistry in and above snow at Summit, Greenland – Part 1: Model description and results, Atmos. Chem. Phys., 11, 4899–4914, doi:10.5194/acp-11-4899-2011, https://www.atmos-chem-phys.net/11/4899/2011/, 2011.

Toyota, K., McConnell, J. C., Lupu, A., Neary, L., McLinden, C. A., Richter, A., Kwok, R., Semeniuk, K., Kaminski, J. W., Gong, S. L., Jarosz, J., Chipperfield, M. P., and Sioris, C. E.: Analysis of reactive bromine production and ozone depletion in the Arctic boundary layer using 3-D simulations with GEM-AQ: inference from synoptic-scale patterns, Atmos. Chem. Phys., 11, 3949–3979, doi:10.5194/acp-11-3949-2011, 2011.

US National Snow & Ice Data Center (NSIDC): EASE-Grid Sea Ice Age, online, http://nsidc.org/soac/sea-ice-age-year.html#seaiceagesequential, 2017.

Wesely, M. L.: Parameterization Of Surface Resistances To Gaseous Dry Deposition In Regional-Scale Numerical-Models, Atmos. Environ., 23, 1293–1304, doi:10.1016/0004-6981(89)90153-4, 1989.

Yang, X., Pyle, J. A., Cox, R. A., Theys, N., and Van Roozendael, M.: Snow-sourced bromine and its implications for polar tropospheric ozone, Atmos. Chem. Phys., 10, 7763–7773, doi:10.5194/acp-10-7763-2010, 2010.

Ziska, F., Quack, B., Abrahamsson, K., Archer, S. D., Atlas, E., Bell, T., Butler, J. H., Carpenter, L. J., Jones, C. E., Harris, N. R. P., Hepach, H., Heumann, K. G., Hughes, C., Kuss, J., Krüger, K., Liss, P., Moore, R. M., Orlikowska, A., Raimund, S., Reeves, C. E., Reifenhäuser, W., Robinson, A. D., Schall, C., Tanhua, T., Tegtmeier, S., Turner, S., Wang, L., Wallace, D., Williams, J., Yamamoto, H., Yvon-Lewis, S., and Yokouchi, Y.: Global sea-to-air flux climatology for bromoform, dibromomethane and methyl iodide, Atmos. Chem. Phys., 13, 8915–8934, doi:10.5194/acp-13-8915-2013, 2013.